Polyfunctional phosphine ligands
II. Iridium(I) complexes of the 7-diphenylphosphino-2,4-dimethyl-1,8-naphthyridine (dpnapy) ligand. X-ray crystal structure of [{Ir(cod)Cl}$_2$(μ-dpnapy)]

Sandra Lo Schiavo[a,*], Maria Grassi[b], Giovanni De Munno[c], Francesco Nicolò[a]
and Giuseppe Tresoldi[a]

[a]*Dipartimento di Chimica Inorganica, Analitica e Struttura Molecolare, Università di Messina, Salita Sperone no 31, 98166 Vill S Agata, Messina (Italy)*
[b]*Dipartimento di Chimica Inorganica e Metallorganica, Università di Milano, via Venezian 21, I-20133 Milan (Italy)*
[c]*Dipartimento di Chimica, Università della Calabria, 87030 Arcavacata di Rende, Cosenza (Italy)*

(Received June 29, 1993; revised October 19, 1993)

Abstract

The coordination chemistry of the polyfunctional phosphine ligand, 7-diphenylphosphino-2,4-dimethyl-1,8-naphthyridine (dpnapy) with iridium(I) complexes has been investigated. Dpnapy reacts with *cis*-[Ir(CO)$_2$(*p*-toluidine)Cl] in 1:2 and 1:1 molar ratios giving the P-monodentate containing ligand complexes *trans*-[Ir(CO)(dpnapy)$_2$Cl] (**1**) and *cis*-[Ir(CO)$_2$(dpnapy)Cl] (**2**), respectively. Complex **2** is unstable in solution; IR and ^{31}P NMR spectroscopic data show at r.t. it transforms into **1** in a short time. The reaction of dpnapy with [{Ir(cod)Cl}$_2$] (cod = cycloocta-1,5-diene) also depends on the metal to ligand ratio used. The mononuclear complex [Ir(cod)(dpnapy)Cl] (**3**), containing P-coordinated dpnapy, is obtained from the 1.2 dimer:ligand reaction. The ^{1}H and ^{13}C NMR spectra of **3** are temperature dependent. They show that the fluxional behaviour involves the cod ligand and is explained by the formation of a labile five-coordinate intermediate displaying a fast exchange of the non-equivalent cod protons and carbons. Treatment of **3** with AgClO$_4$ leads to a species, formulated on the basis of IR and analytical data, as [{Ir(cod)(dpnapy)}ClO$_4$] (**4**) in which dpnapy is very likely P–N(8) chelated The binuclear complex [{Ir(cod)Cl}$_2$(μ-dpnapy)] (**5**), containing a bridging bidentate dpnapy, is obtained from the 1.1 [{Ir(cod)Cl}$_2$]:dpnapy reaction. The bridging function of dpnapy is realized through the phosphorus and the terminal nitrogen binding sites in agreement with the NMR data and as confirmed by an X-ray analysis Complex **5** crystallizes into the monoclinic space group $P2_1/n$ with cell parameters $a = 17.813(4)$, $b = 12.339(3)$, $c = 18\,221(5)$ Å, $\beta = 106.73(2)°$ and with $Z = 4$. The structure model, with all the non-H atoms anisotropic, was refined up to $R = 0.040$ and $R_w = 0.050$ with the goodness-of-fit = 0.91. The asymmetric unit contains one discrete molecule constitued by two independent square-planar iridium moieties, considering each ethylenic system of cycloocta-1,5-diene like a unique coordination site. No interaction exists between the two iridium metal centres

Key words Iridium complexes, Polyfunctional ligand complexes; Phosphine complexes; Crystal structures

Introduction

Considerable attention is today devoted to the design and synthesis of polydentate ligands as the backbone for multicentred metal complexes. In this context we have synthesized the ligand, 7-diphenylphosphino-2,4-dimethyl-1,8-naphthyridine [1] (dpnapy) (Fig. 1), a new polyfunctional phosphine ligand characterized by a rigid skeleton and a quasi-linear disposition of the phosphorus and the two nitrogen binding sites.

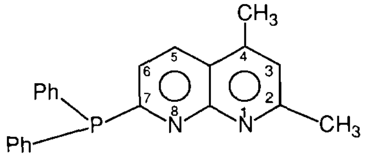

Fig 1 7-Diphenylphosphino-2,4-dimethyl-1,8-naphthyridine

Our previously investigation on its coordination chemistry towards some rhodium(I) [1] complexes showed that dpnapy may act as a P-monodentate or a bridging bidentate ligand utilizing the P and the terminal nitrogen

---

*Author to whom correspondence should be addressed.

SSDI 0020-1693(93)03730-X

N(1) atoms. Furthermore, according with its geometric features dpnapy is able to produce metallocycles, that, in some cases, are precursors of trinuclear metal arrays [2, 3]. It reacts, in fact, with $[\{Rh(CO)_2Cl\}_2]$ giving the twelve-membered metallocycle $[\{Rh(CO)(\mu\text{-dpnapy})Cl\}_2]$, which, as revealed by an X-ray diffraction study, does not display the right geometrical features to allow inclusion of other metal ions in the central cavity.

As a continuation of our studies on the coordination chemistry of dpnapy, we planned a systematic investigation of its reactivity with a series of d^8-metal complexes [4] aimed at the synthesis of metallocycles suitable for inclusion chemistry. In this paper we report the synthesis and NMR solution behaviour of some iridium(I) complexes of dpnapy. The X-ray crystal structure of the complex $[\{Ir(cod)Cl\}_2(\mu\text{-dpnapy})]$ is also described.

Experimental

General data

The 7-diphenylphosphino-2,4-dimethyl-1,8-naphthyridine (dpnapy) ligand was prepared as previously described [1]. The *cis*-$[Ir(CO)_2(p\text{-toluidine})Cl]$ complex was prepared by a literature method [5]. The other reagents were commercially obtained and used as supplied. All reactions were carried out under an atmosphere of nitrogen. IR spectra were recorded on KBr or CsI pellets with a Perkin-Elmer FT 1720X spectrometer. The NMR measurements were made on Bruker AC-200 and Varian XL-200 spectrometers using standard pulse sequencies [6]. Conductivity data were obtained with a Radiometer CDM 3 conductivity meter. Molecular weights were determined with a Knauer vapour-pressure osmometer. Elemental analyses were performed by Malissa-Reuter Mikroanalytisches Laboratorium, Elbach, Germany, and REDOX snc laboratorio microanalisi, Cologno Monzese, Milan, Italy.

Preparations

trans-[Ir(CO)(dpnapy)₂Cl] (1)

Solid dpnapy (0.175 g, 0.152 mmol) was added to a stirred benzene solution (30 cm^3) of *cis*-$[Ir(CO)_2(p\text{-toluidine})Cl]$ (0.100 g, 0.256 mmol). Stirring was continued for 1 h, during which time compound **2** precipitated as a dark yellow solid. n-Hexane (30 cm^3) was added to complete the precipitation of the product. The mother liquors were pipetted off and the solid washed several times with diethyl ether (4×10 cm^3). Yield 78% (0.188 g, 0.200 mmol). *Anal.* Found: C, 57.50; H, 4.11; N, 5.91; Cl, 3.81; P, 6.62. Calc. for $C_{45}H_{38}N_4ClOP_2Ir$: C, 57.47; H, 4.07; N, 5.96; Cl, 3.77; P, 6.59%. IR (nujol mulls, CsI): ν(CO) 1957, ν(Ir–Cl) 329 cm^{-1}.

cis-[Ir(CO)₂(dpnapy)Cl] (2)

Solid dpnapy (0.062 g, 0.018 mmol) was added to a stirred benzene solution (40 cm^3) of *cis*-$[Ir(CO)_2(p\text{-toluidine})Cl]$ (0.07 g, 0.179 mmol). Stirring was continued for 30 min. On addition of n-hexane (40 cm^3) compound **1** precipitated as a lemon–yellow solid. The mother liquors were pipetted off, the solid washed with diethyl ether (2×10 cm^3) and dried *in vacuo*. Yield 75% (0.084 g, 0.0134 mmol). *Anal.* Found: 46 11; H, 3.11; N, 4.41; Cl, 5.89; P, 4.98. Calc. for $C_{24}H_{19}N_2ClPO_2Ir$: C, 46.04, H, 3.06; N, 4.47; Cl, 5.66; P, 4.95%. IR (nujol mulls, CsI): ν(CO) 2062, 1978, ν(Ir–Cl) 320 cm^{-1}. IR ($CHCl_3$): ν(CO): 2070, 1966 cm^{-1}.

[Ir(cod)(dpnapy)Cl] (3)

Procedure a. A solution of dpnapy (0.070 g, 0.203 mmol) and $[\{Ir(cod)Cl\}_2]$ (0.068 g, 0.101 mmol) in CH_2Cl_2 (30 cm^3) was stirred for about 10 min. Then n-hexane was added inducing the precipitation of compound **3** as a light-orange solid. It was washed with diethyl ether and dried *in vacuo*. Yield 88% (0.120 g, 0.178 mmol).

Procedure b. Solid dpnapy (0.034 g, 0.100 mmol) was added to a dichloromethane solution (30 cm^3) of $[\{Ir(cod)Cl\}_2(\mu\text{-pnapy})]$ (**5**) (0.101 g, 0.100 mmol) and the resulting mixture left to stir for 30 min. By addition of n-hexane compound **3** precipitated in a nearly quantitative amount (0.034 g, 0.057 mmol). *Anal.* Found: C, 53.55; H, 4.71; N, 4.21; Cl, 5.31; P, 4.60. Calc. for $C_{30}H_{31}ClN_2PIr$: C, 53.13; H, 4.61; N, 4.13; Cl, 5.23; P, 4.57%. IR (nujol, CsI): ν(Ir–Cl) 302 cm^{-1}.

[Ir(cod)(pnapy)]ClO₄ (4)

Procedure a. $AgClO_4$ (0.025 g, 0.120 mmol) was added to a stirred acetone solution (30 cm^3) of [Ir(cod)(pnapy)Cl] (**3**) (0.080 g, 0.118 mol). AgCl was immediately formed. It was filtered and the resulting solution reduced in volume (*c.* 10 cm^3). By addition of diethyl ether (20 cm^3) complex **4** precipitated as a pale yellow solid. Yield 0.058 g (0.078 mmol), 60%.

Procedure b. $AgClO_4$ (0.061 g, 0.296 mmol) was added to a stirred acetone solution (30 cm^3) of $[\{Ir(cod)Cl\}_2]$ (0.100 g, 0.148 mmol). Immediately solid AgCl precipitated. It was filtered off and to the filtrate solid dpnapy (0.139 g, 0.406 mmol) was added. The resulting mixture was left to stir for about 10 min and then diethyl ether (40 cm^3) was added to induce the precipitation of the compound. Yield 0.151 g (0.272 mmol), 70%. *Anal.* Found: C, 49.01; H, 2.80; N, 3.79; Cl, 4.88; P, 4.15. Calc. for $C_{30}H_{21}N_2ClO_4PIr$: C, 49.22; H, 2.89; N, 3.83; Cl, 4.84; P, 4.23%. IR (nujol mulls, KBr): ν(Cl–O) 1100 cm^{-1}.

[{Ir(cod)Cl}$_2$(μ-pnapy)] (5)

Procedure a. A CH_2Cl_2 solution (40 cm^3) of dpnapy (0.044 g, 0.130 mmol) and [{Ir(cod)Cl}$_2$] (0.087 g, 0.130 mmol) was stirred for 20 min. The solution, initially yellow, turned orange. By addition of n-hexane compound **5** precipitated as a yellow-orange solid. It was filtered off and washed with diethyl ether. Recrystallization from dichloromethane/diethyl ether (1/1) (30 cm^3) gave **5** as orange crystals in 95% yield (0.125 g, 0.123 mmmol).

Procedure b. Solid [{Ir(cod)Cl}$_2$] (0.087 g, 0.130 mmol) was added to a dichloromethane (40 cm^3) solution of [Ir(cod)(pnapy)Cl] (**3**) (0.176 g, 0.260 mmol). Soon the yellow starting colour solution turned orange. The resulting mixture was left to stir for *c.* 10 min, then n-hexane (40 cm^3) was added inducing the precipitation of the compound. Yield 0.108 g, 82%. *Anal.* Found: C, 54.85; H, 5.26; N, 3.38; Cl, 8.64. Calc for $C_{38}H_{43}N_2Cl_2PIr_2$: C, 45.01; H, 4.27; N, 2.76; Cl, 6.99; P, 3.05%. IR (nujol, CsI): ν(Ir–Cl) 300, 285 cm^{-1}. *M*, 985 (CH_2Cl_2) (calc. 1014).

X-ray data collection and structure refinement

Red–orange crystals of [{Ir(cod)Cl}$_2$(μ-dpnapy)] (**5**) were obtained by layering diethyl ether over a CH_2Cl_2 solution of the complex. Diffraction data were collected at 298 K with a Siemens R3m/V automatic four-circle diffractometer, using graphite-monochromated Mo Kα radiation ($\lambda = 0.71073$ Å). Information concerning crystallographic data collection and refinement of the structure is listed in Table 1. The unit-cell parameters were obtained from least-squares refinement of the setting angles of 25 reflections in the 2θ range 15–30°. A total of 10 882 reflections was collected by the variable-speed ω–2θ scan method in the 2θ range 3–55° with index ranges $-6 \leqslant h \leqslant 23$, $-6 \leqslant k \leqslant 16$, $-23 \leqslant l \leqslant 22$. 8792 of them were unique and, from these, 4323, were assumed as observed ($I > 7\sigma(I)$) and used for the refinement of the structure. Three standard reflections, monitored after every 100 reflections, showed no sign of crystal deterioration. Lorentz–polarization and ψ-scan absorption correction [7] were applied to the intensity data. Maximum and minimum transmission factors were 0.046 and 0.016.

The structures were solved by standard Patterson methods with SHELXTL PLUS program [8] and subsequently completed by Fourier recycling. All non-hydrogen atoms were refined anisotropically. The hydrogen atoms of dpnapy were set in calculated position and refined as riding atoms, assuming a common fixed isotropical thermal parameter. The final full-matrix least-squares refinement, minimizing the function $\Sigma w(|F_o|-|F_c|)^2$ with $w = 1.0000/[\sigma^2(F_o)+0.0018(F_o)^2]$, converged at *R* and R_w indices of 0.0401 and 0.0503. The ratio reflections/(number of variable parameters) was 10.6. Solutions and refinements were performed with the SHELXTL PLUS system [8]. The final geometrical calculations were carried out with the PARST program [9]. The drawings were performed using the XP utility of the SHELXTL PLUS system. The final atomic coordinates for non-hydrogen atoms and selected bond lengths and angles are given in Tables 2 and 3. See also 'Supplementary material'.

TABLE 1 Crystal data and structure determination summary

Formula	$C_{38}H_{43}Cl_2Ir_2N_2P$
Crystal system	monoclinic
Space group	$P2_1/n$
Unit cell dimensions	
a (Å)	17.813(4)
b (Å)	12 339(3)
c (Å)	18 221(5)
β (°)	106.73(2)
V (Å^3)	3835 3(17)
Z	4
Molecular weight	1014 0
D_{calc} (g cm^{-3})	1 756
Linear absorption coefficient (mm^{-1})	7.141
F(000)	1952
2θ Range (°)	3.0 to 55 0
Scan type	2θ–ω
Scan speed (variable) (° min^{-1})	2.5–5 in ω
Scan range, ω (°)	1.40 plus Kα separation
Reflections measured	10882
Unique reflections ($R_{int} = 0.007$)	8792
Observed reflections ($F \geqslant 7\sigma(F)$) (m)	4323
No refined parameters (*n*)	406
Weighting scheme	$w^{-1} = \sigma^2(F) + 0.0018F^2$
$R = \Sigma\|F_o - F_c\|/\Sigma F_o$	0.040
$R_w = \Sigma w\|F_o - F_c\|/\Sigma w F_o$	0.050
$G = (\Sigma w(F_o - F_c)^2/(m-m))^{1/2}$	0 91

Results and discussion

All the complexes were characterized by elemental analyses, IR, and multinuclear NMR spectroscopy. IR and analytical data are reported in 'Experimental'. Significant ^{1}H and ^{13}C, and ^{31}P{^{1}H} NMR data are given in Tables 4 and 5, respectively.

Reactions of dpnapy with cis-[Ir(CO)$_2$(p-toluidine)Cl]

The mononuclear complexes *trans*-[Ir(CO)(dpnapy)$_2$Cl] (**1**) and *cis*-[Ir(CO)$_2$(dpnapy)Cl] (**2**) containing P-coordinated dpnapy are the products of the reactions with *cis*-[Ir(CO)$_2$(*p*-toluidine)Cl] in the molar ratio 2:1 and 1:1, respectively.

By addition of dpnapy to a benzene solution of *cis*-[Ir(CO)$_2$(*p*-toluidine)Cl] (molar ratio 2:1) the complex *trans*-[Ir(CO)(P-PNN)$_2$Cl] (**1**) precipitates as a dark yellow solid in high yield. **1** is an air-sensitive solid, sparingly soluble only in chlorinated solvents. The above

TABLE 2. Atomic coordinates ($\times 10^4$) and equivalent isotropic displacement coefficients ($Å^2 \times 10^3$) for the non-hydrogen atoms

	x	y	z	U_{eq}[a]
Ir(1)	1146(1)	1223(1)	2138(1)	48(1)
Ir(2)	−2239(1)	2072(1)	3793(1)	38(1)
Cl(1)	1968(2)	1591(3)	3377(2)	65(1)
Cl(2)	−1535(2)	3149(3)	4840(2)	54(1)
P	51(2)	1778(2)	2480(2)	39(1)
N(1)	−1520(5)	716(7)	4245(5)	34(3)
C(2)	−1680(6)	82(8)	4787(6)	37(4)
C(3)	−1331(6)	−917(9)	4989(6)	40(4)
C(4)	−791(6)	−1329(8)	4677(6)	37(4)
C(5)	41(6)	−909(9)	3805(6)	39(4)
C(6)	223(6)	−194(9)	3312(6)	38(4)
C(7)	−191(6)	808(8)	3150(5)	34(3)
N(8)	−753(5)	1062(6)	3452(4)	33(3)
C(9)	−930(6)	378(8)	3945(5)	29(3)
C(10)	−549(6)	−650(8)	4159(5)	31(3)
C(11)	−456(7)	−2439(9)	4875(7)	45(4)
C(12)	−2276(7)	506(10)	5161(7)	52(5)
C(13)	−853(7)	1842(9)	1705(6)	40(4)
C(14)	−1326(7)	945(10)	1468(6)	45(4)
C(15)	−1970(7)	984(11)	811(7)	52(4)
C(16)	−2127(8)	1942(12)	380(7)	64(5)
C(17)	−1658(9)	2827(12)	616(8)	71(6)
C(18)	−1043(8)	2802(10)	1263(7)	57(5)
C(19)	112(7)	3100(8)	2959(6)	40(4)
C(20)	777(8)	3730(12)	3073(10)	75(7)
C(21)	842(10)	4678(13)	3478(11)	86(8)
C(22)	240(10)	5053(10)	3719(9)	72(6)
C(23)	−429(8)	4452(10)	3600(7)	54(5)
C(24)	−503(7)	3499(9)	3212(7)	48(4)
C(25)	2094(10)	220(19)	1940(11)	96(8)
C(26)	2188(11)	1290(26)	1721(10)	117(11)
C(27)	1929(15)	1565(31)	908(13)	208(22)
C(28)	1164(13)	1509(22)	486(11)	126(12)
C(29)	614(9)	1267(19)	952(8)	88(8)
C(30)	456(10)	280(16)	1203(9)	81(7)
C(31)	908(11)	−737(16)	1106(13)	109(10)
C(32)	1787(14)	−614(24)	1354(16)	191(17)
C(33)	−2704(7)	1334(10)	2712(6)	51(4)
C(34)	−3107(7)	990(11)	3183(7)	57(5)
C(35)	−3925(8)	1326(13)	3210(9)	74(6)
C(36)	−3995(8)	2569(12)	3220(9)	66(6)
C(37)	−3230(7)	3099(11)	3590(8)	56(5)
C(38)	−2696(8)	3472(10)	3185(8)	59(5)
C(39)	−2824(10)	3318(14)	2320(8)	80(7)
C(40)	−3037(10)	2154(13)	2067(7)	74(6)

[a] Equivalent isotropic U defined as one third of the trace of the orthogonalized U_{ij} tensor

TABLE 3 Selected bond lengths (Å) and bond angles (°)[a]

Ir(1)–Cl(1)	2.354(3)	Ir(2)–Cl(2)	2.366(3)
Ir(1)–P	2.314(3)	Ir(2)–N(1)	2.122(8)
Ir(1)–X(01)	2.09(2)	Ir(2)–X(03)	1.976(9)
Ir(1)–X(02)	2.00(1)	Ir(2)–X(04)	1.998(8)
Ir(1)–C(25)	2.20(2)	Ir(2)–C(33)	2.11(1)
Ir(1)–C(26)	2.20(2)	Ir(2)–C(34)	2.10(1)
Ir(1)–C(29)	2.09(1)	Ir(2)–C(37)	2.12(1)
Ir(1)–C(30)	2.14(2)	Ir(2)–C(38)	2.09(1)
C(25)–C(26)	1.40(4)	C(33)–C(34)	1.34(2)
C(25)–C(32)	1.47(3)	C(33)–C(40)	1.53(2)
C(26)–C(27)	1.45(3)	C934)–C(35)	1.53(2)
C(27)–C(28)	1.37(3)	C(35)–C(36)	1.54(2)
C(28)–C(29)	1.50(3)	C(36)–C(37)	1.48(2)
C(29)–C(30)	1.37(3)	C(37)–C(38)	1.44(2)
C(30)–C(31)	1.53(3)	C(38)–C(39)	1.54(2)
C(31)–C(32)	1.51(3)	C(39)–C(40)	1.52(2)
P–C(7)	1.87(1)	P–C(13)	1.81(1)
P–C(19)	1.84(1)		
X(01)–Ir(1)–X(02)	86.1(5)	X(03)–Ir(2)–X(04)	87.5(4)
P–Ir(1)–X(02)	94.2(4)	N(1)–Ir(2)–X(04)	90.9(4)
P–Ir(1)–X(01)	178.8(5)	N(1)–Ir(2)–X(03)	176.4(4)
Cl(1)–Ir(1)–X(02)	173.3(4)	Cl(2)–Ir(2)–X(04)	175.4(3)
Cl(1)–Ir(1)–X(01)	88.3(4)	Cl(2)–Ir(2)–X(03)	90.8(3)
Cl(1)–Ir(1)–P	91.5(1)	Cl(2)–Ir(2)–N(1)	90.6(2)
Ir(1)–P–C(19)	116.9(4)	Ir(1)–P–C(13)	115.7(4)
Ir(1)–P–C(7)	111.1(4)	C(13)–P–C(19)	104.5(5)
C(7)–P–C(19)	104.6(5)	C(7)–P–C(13)	102.6(5)

[a] The symbols X(01), X(02), X(03), X(04) represent the middle points of the ethylenic bonds C(25)–C(26), C(29)–C(30), C(33)–C(34), C(37)–C(38), respectively

TABLE 4 ^1H and ^{13}C NMR data[a]

	Me_2	Me_4	CH(cod)	CH_2(cod)
^1H NMR				
dpnapy[b]	2.73	2.62		
1[b]	2.78	2.61		
2[c]	2.75	2.62		
3[b]	2.75	2.54	5.4, 2.9	1.5–2.5
5[d]	3.56	2.57	5.35, 5.1 4.6, 4.3, 3.6, 3.0 (2H), 2.6	1.5–2.4
^{13}C NMR				
dpnapy[b]	25.60	17.95		
1[b]	25.88	18.22		
2[c]	26.18	18.21		
3[c]	26.2	18.7	94.7, 54.3	33.6, 29.8
5[c, d]	27.8	18.7	95.6, 94.5, 67.3, 62.8, 60.5, 59.2, 55.8, 54.2	30.1, 34.5

[a] At 200.13 (^1H) and 50.323 (^{13}C) MHz, chemical shifts (δ) in ppm referred to $SiMe_4$, 298 K. [b] $CDCl_3$ [c] CD_2Cl_2 [d] 223 K

formulation was substantiated by analytical, IR and NMR spectroscopic data. The IR spectrum (nujol mulls) exhibits the carbonyl and Ir–Cl absorptions at 1957 and 329 cm^{-1}, respectively. As expected the ^1H and ^{13}C NMR spectra, obtained by mixing the reagents in an NMR tube at r.t., appear analogous to those of the free ligand and other mononuclear complexes containing P-bonded dpnapy [1]. The ^{31}P spectrum consists of a sharp band at 6.12 ppm and does not change by lowering the temperature as well as by adding an excess of dpnapy. Both these experiments exclude a phosphine dissociation process.

TABLE 5 $^{31}P\{^{1}H\}$ NMR data[a]

Compound	T (K)	δ
dpnapy[b]	298	−1.1
1[b]	298	6.12
2[c]	223	12.30
3[c]	298	21.07
5[c]	298	19.90
	198	25.04
		16.17

[a]At 81.015 MHz, δ in ppm referred to external H_3PO_4 [b]In $CDCl_3$. [c]In CD_2Cl_2

The compound *cis*-[Ir(CO)$_2$(dpnapy)Cl] (**2**) is obtained as a lemon–yellow air-sensitive solid by treatment of *cis*-[Ir(CO)$_2$(*p*-toluidine)Cl] with one equivalent of dpnapy in benzene solution. Consistent with this formulation the IR spectrum (nujol mulls) shows two carbonyl stretches at 2062 and 1982 cm^{-1}, indicative of the *cis*-disposition of the carbonyl groups while the Ir–Cl stretch is observed at 320 cm^{-1}. Complex **2** in solution undergoes some chemical changes. By studying the spectral modifications occurring in the carbonyl region of the IR spectrum of a CH_2Cl_2 sample of **2**, it was observed that in a short time (*c*. 15 min) the two ν(CO) starting bands (2070 and 1966 cm^{-1}) disappear and are replaced by a new one at 1967 cm^{-1} (1957 cm^{-1} in solid). The same modification has been detected by ^{31}P NMR spectroscopy. Complex **2** which initially shows a broad absorption at *c*. 12 ppm (CD_2Cl_2, r.t.), with time, transforms into a species exhibiting a sharp resonance at 6.14 ppm and ν(CO) at 1967 cm^{-1}.

In order to elucidate this process a CD_2Cl_2 sample of **1** was prepared by mixing the reactants at low temperature in an NMR tube and its evolution followed by variable temperature ^{31}P NMR spectra. (Much care was taken in this experiment to avoid an excess of dpnapy. When this happens complex **1** readily precipitates). The ^{31}P spectrum at 223 K exhibits a main band at 12.3 ppm, very likely due to *cis*-[Ir(CO)$_2$(dpnapy)Cl] (**2**), and one of low intensity at 6.12 ppm. On warming the resonance at 12.30 ppm slowly disappears while that at 6.12 ppm sharpens up The CD_2Cl_2 reaction mixture taken to dryness gives in the IR spectrum only one C–O stretching at 1957 cm^{-1}. ^{1}H and ^{13}C NMR spectra remain unchanged over the same range of temperature and do not display downfield shifts for the 2-Me protons and carbon absorptions with respect to those of the free ligand. This excludes that **2** may transform into a metallocycle, occasionally exhibiting the resonance at *c*. 6 ppm, containing two Ir(CO)Cl units and two dpnapy molecules in a head-to-tail arrangement (see below). On the other hand comparison of the IR and ^{31}P NMR spectral data of complex **2** with those of **1** suggests that complex **2** in solution transforms, through an unknown mechanism, into **1**.

This study shows that *trans*-[Ir(CO)(dpnapy)$_2$Cl] (**1**) is the main product of the reactions of dpnapy with *cis*-[Ir(CO)$_2$(*p*-toluidine)Cl] and that dpnapy fails to give a metallocycle like [Rh(CO)(μ-dpnapy)Cl]$_2$, that, on the contrary was the only product obtained from the analogous reactions with [{Rh(CO)$_2$Cl}$_2$]. These results may be due to the combination of several factors: (i) the weaker Ir–N bond strength with respect to Rh–N, (ii) the bigger difference in Ir–N and Ir–P bond strengths relative to Rh–N and Rh–P; (iii) the stable arrangement of the ligands around the iridium centre derived from the *trans* arrangement of the two phosphorus atoms and the CO and Cl ligands, respectively [10].

To substantiate these suppositions unreacted *trans*-[Ir(CO)(dpnapy)$_2$Cl] (**1**) and the metallocycle [Rh(CO)(μ-dpnapy)Cl]$_2$ were obtained from the reactions of *trans*-[Ir(CO)(dpnapy)$_2$Cl] (**1**) with *cis*-[Ir(CO)$_2$(*p*-toluidine)Cl] and [{Rh(CO)$_2$Cl}$_2$], respectively.

Reactions of dpnapy with [Ir(cod)Cl]$_2$

It is well known that the reactions of polydentate ligands with [{M(cod)Cl}$_2$] (M = Rh, Ir) occur by cleavage of the chlorine bridges leading to different types of compounds the nature of which is dependent on the geometrical features of the ligand, solvent and stoichiometric ratio employed [11].

In accordance with these findings dpnapy reacts with [{Ir(cod)Cl}$_2$] giving products the nature of which is dependent on (i) the ligand to metal ratio and (ii) the rigid skeleton of the ligand. The complexes [Ir(cod)(dpnapy)Cl] (**3**) and [{Ir(cod)Cl}$_2$(μ-dpnapy)] (**5**) are the products obtained when the 1/2 and 1/1 stoichiometry, respectively, is used (Scheme 1).

Both the complexes are orange, air-unstable solids which dissolve easily in chlorinated solvents.

Complex **3**, in which dpnapy is P-coordinated, can be alternatively obtained by reacting [{Ir(cod)Cl}$_2$(μ-dpnapy)] (**5**) with the equivalent amount of dpnapy. The ^{31}P NMR spectrum displays a band at 21.07 ppm while the ^{1}H and ^{13}C NMR ($CDCl_3$) spectra are temperature dependent. At r.t. they show the resonances related to the dpnapy moiety and no signals in the olefinic cod region. By lowering the temperature (223 K) two signals emerge at 5.4 and 2.9 ppm in the proton and at 94.7 and 54.3 ppm in the carbon spectrum,

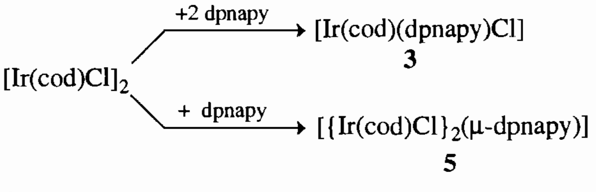

Scheme 1.

respectively, suggesting that a further rapid interchange of olefinic cod protons and carbons is still operating at low temperature, otherwise four signals would be observed instead of two.

The observed fluxionality is common to many square-planar cycloocta-1,5-diene d^8 complexes. It is usually attributed to the formation of stereochemically non-rigid penta-coordinated intermediates (displaying a fast exchange of the non-equivalent cod protons and carbons) originating from an intermolecular [12, 13] or an intramolecular association equilibrium process [11, 14]. A similar dynamic NMR process was found and discussed in detail for the analogous rhodium complex [1]. In this case the geometrical features and the polydentate nature of dpnapy led us to suggest that in the formation of the labile five-coordinated intermediate an intramolecular associative mechanism, realized via attack of N(8) on the metal, is favoured Comparison of the ^{1}H and ^{13}C NMR low temperature spectra of **3** with those of the corresponding rhodium complex indicates that the fluxional process observed for **3** may occur through the same mechanism.

Treatment of [Ir(cod)(dpnapy)Cl] (**3**) with an equimolar amount of $AgClO_4$ affords a species formulated, on the basis of IR and analytical data, as [Ir(cod)(dpnapy)]ClO_4 (**4**) in which dpnapy is very likely chelated via P–N(8) This complex is very unstable in solution and transforms rapidly into unidentified species preventing its full spectroscopic characterization. Geometric constraints of dpnapy can account for the instability of the complex in solution. The fixed and linear disposition of the phosphorus and two nitrogen binding sites makes the four-membered chelate ring realized via P–N(8) coordination to iridium unstable. This is in keeping with the literature reports on 2-(diphenylphosphino)pyridine that rarely adopts a chelating coordination mode [15].

[{Ir(cod)Cl}$_2$] reacts with dpnapy in the 1:1 molar ratio giving the binuclear complex [{Ir(cod)Cl}$_2$(μ-dpnapy)] (**5**), in which dpnapy, acting as a bridging bidentate ligand, coordinates two Ir(cod)Cl moieties by the P and N(1) atoms. Such a formulation was assigned on the basis of analytical, conductivity and NMR data. An X-ray diffraction analysis confirmed that this structure is retained in the solid state. In agreement with the proposed structure the ^{1}H and ^{13}C NMR spectra display eight peaks for the cod olefinic protons and carbons (Fig. 2) while the signals related to the 2-Me protons (3.56 ppm) and carbon (27.80 ppm) appear downfield shifted with respect to free dpnapy (^{1}H, 2.73; ^{13}C, 25.60 ppm). As already found for the rhodium complexes the shift of the α-proton and carbon atoms of dpnapy experiences its coordination also through N(1) and is explained in terms of magnetic anisotropy of the metal [16].

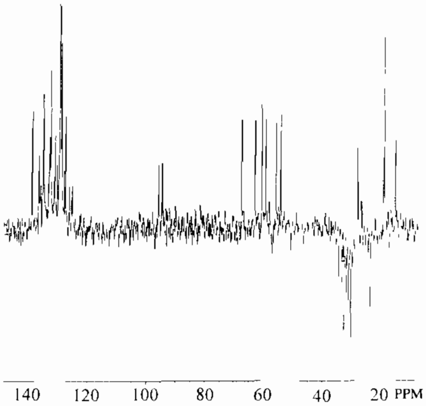

Fig. 2. ^{13}C NMR spectra for complex **4** (50 232 MHz, CD_2Cl_2, 298 K)

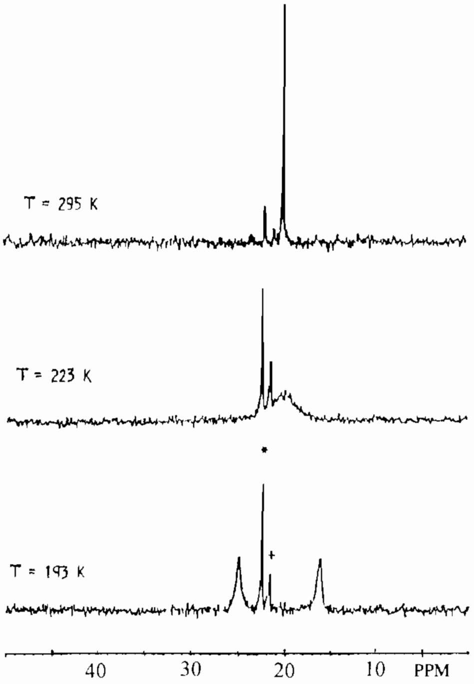

Fig. 3. Variable ^{31}P NMR spectra (81 015 MHz, CD_2Cl_2) for complex **5**, * due to traces of complex **3** and $^+$ of dpnapy oxide

The variable ^{31}P NMR spectra have revealed that complex **5** is also involved in a dynamic process. The ^{31}P spectrum at r.t. consists of a single resonance at 19.90 ppm which at 228 K coalesces. A further lowering of the temperature (198 K) causes the appearance of two signals (25.04 and 16.17 ppm), which by analogy to the related rhodium complex [1] may be assigned to two stereoisomers rapidly interchanging at r.t. (Fig. 3).

X-ray structure description of [{Ir(cod)Cl}$_2$(μ-dpnapy)] (5)

The asymmetric unit of the cell is composed of one discrete molecule containing two iridium atoms bridged by the dpnapy ligand, as shown in Fig. 4.

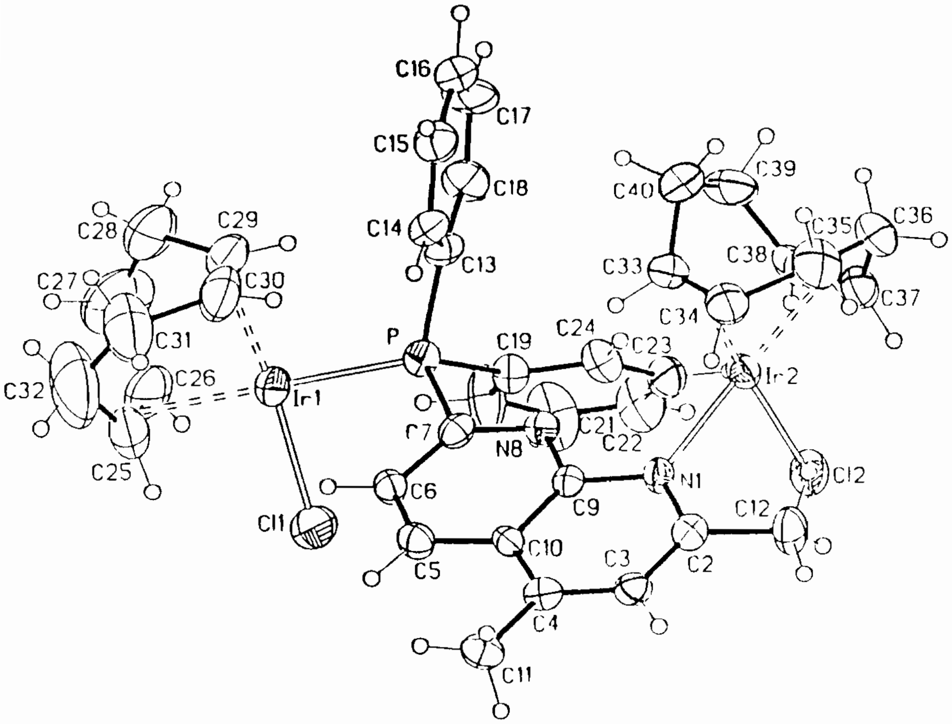

Fig. 4. Perspective view of the molecular unit showing the numbering scheme Thermal ellipsoids are drawn at 40% of probability while hydrogen size is arbitrary The interactions between the iridium atoms and the ligand ethylenic systems are represented conventionally by dotted lines with their corresponding middle points.

The geometry of the dinuclear complex is mainly determined by the rigid planar naphthyridyl fragment of the ligand which coordinates the two iridium atoms through its phosphorus and the more external nitrogen atom, N(1). Considering only the bridging action of the ligand and one metal atom already coordinated to the phosphorus of the diphenylphosphine side, a second 'heavy' atom might be bonded to one of the two nitrogens of the naphthyridyl fragment. If the coordination site is N(8), the bite of the bridging ligand is very small (2.73 Å) and forces the two metal centres to a short internuclear distance, enough to cause a bond interaction commonly observed for the bridging 2-(diphenylphosphino)pyridine ligand [17–19]. Further it is possible to bond the second metal by the N(1) atom, in such a case the ligand bite is noticeably larger (5.01 Å) and then the bigger centre separation does not allow a metal–metal bond, like that found in the title compound which shows an Ir···Ir distance of 7.55 Å.

Each of the two atoms Ir(1) and Ir(2), coordinated to the atoms P and N(1), respectively, of the bridging ligand, is bonded to a chlorine atom and the two ethylenic fragments of a cycloocta-1,5-diene. Therefore, considering the cyclooctadiene as a chelating ligand with the two coordination sites represented by the middle points of the two double bonds, each iridium shows an almost perfect square-planar coordination geometry with the C_8H_{12} cycle folded in such a way the angle middle-(1)–metal–middle-(2) is close to 90° (86.11(5) and 87.54(4)°, respectively), in complete accordance with the very similar arrangement observed for [(2-diphenylphosphino)pyridine-P)-chloro-(η^4-cyclo-octa-1,5-diene)-iridium] [20]. Each centre and its four coordination sites so defined lie quite perfectly on a plane which is disposed almost orthogonally to the mean plane of the naphthyridyl fragment. Apart from the obviously different Ir(1)–P and Ir(2)–N(1) bond distances, the geometry of the two centres is very similar but, in spite of the equal value of the two Ir–Cl lengths, a slight difference is observed between the two average values for the four Ir–$C_{\text{ethylenic}}$ distance set (2.16(2) versus 2.11(1) Å). This discrepancy seems to be mainly due to an electron *trans*-effect of the phosphorus, as shown by the significantly longer Ir(1)–C distance with C(25) and C(26) (2.20(2) Å) opposite to P with respect to the other six Ir–C lengths (average 2.11(2) Å). A modelling study of the steric hindering of the bridging ligand on the two metal coordination shells pointed out a lower action on Ir(1) through the P-diphenylphosphine fragment than on Ir(2) by the N-naphthyridine side, explaining the less rotated disposition of the Ir(1) coordination plane than of the Ir(2) one with respect to the mean bridging ligand plane (76.94(8) versus 86.16(7)°) from which also Ir(2) is significantly further 0.342(1) versus 0.504(1) Å, respectively, on opposite sides).

Supplementary material

Additional material available from the Cambridge Crystallographic Data Centre comprises H atom coordinates, anisotropic temperature factors and the remaining bond lengths and angles.

Acknowledgements

We thank the Ministero per l'Università e la Ricerca Scientifica e Tecnologica (MURST) and the Consiglio Nazionale delle Ricerche (CNR) for financial support.

References

1 M Grassi, G. De Munno, F. Nicolò and S Lo Schiavo, *J Chem Soc., Dalton Trans*, (1992) 2367

2 A L Balch, *Pure Appl Chem*, *60* (1988) 555, and refs therein

3 A L. Balch, V.J Catalano, M.A Chatfield, J K. Nagle, M M. Olmstead and P E. Reedy, Jr, *J Am Chem Soc*, *113* (1991) 1252

4 S Lo Schiavo, F Nicolò, G. Tresoldi and G De Munno, submitted for publication.

5 U. Klabunde, *Inorg. Synth*, *15* (1974) 82.

6 G A Morris, *Magn Reson. Chem*, *24* (1986) 3H

7 A C.T. North, D.C. Phillips, F S Matheus, *Acta Crystallogr*, *Sect A*, *24* (1968) 351

8 SHELXTL PLUS, Version 3 4, Siemens Analytical X-ray Instruments Inc, Madison WI, 1989

9 M. Nardelli, *Comput Chem*, *7* (1983) 95.

10 M P. Anderson, A L Casalnuovo, B J. Johnson, B.M Mattson, A M Mueting and L H Pignolet, *Inorg Chem*, *27* (1988) 1649.

11 P. Imhoff, R. van Asselt, C J. Elsevier, M C Zoutberg and C H Stam, *Inorg Chim Acta*, *184* (1991) 73, and refs therein.

12 E. Anzuela, M.A. Garralda, R Hernandez, L. Ibarlucea, E Pinilla and M A Monge, *Inorg Chim Acta*, *185* (1991) 211

13 C Volger, K. Vrieze and A.P Praat, *J Organomet Chem*, *14* (1968) 429.

14 H El-Amouri, A.A Bahsun and J.A Osborn, *Polyhedron*, *7* (1988) 2035

15 (a) A. Maisonnet, J.P. Farr, M.M Olmstead, C T Hunt and A.L Balch, *Inorg Chem*, *21* (1982) 3961, (b) J P Farr, M M Olmstead, F.E Wood and A L Balch, *J Am Chem Soc*, *105* (1983) 792; (c) V K. Jain, V.S Jakkal and R Bohra, *J Organomet Chem*, *389* (1990) 417

16 D E Chebi and I.P Rothwell, *Organometallics*, *9* (1990) 2948, and refs therein

17 F A. Cotton and M Matusz, *Inorg Chim Acta*, *45* (1988) 143

18 G Bruno, S. Lo Schiavo, E Rotondo, C G Arena and F Faraone, *Organometallics*, *8* (1989) 886

19 S Lo Schiavo, E Rotondo, G. Bruno and F Faraone, *Organometallics*, *10* (1991) 1613, and refs. therein.

20 P. Lahuerta, I Solana, X. Solans and M Font-Altaba, *J Chem Res*, *33* (1987) 440